



**HAL**  
open science

## Druggable allosteric sites in $\beta$ -propeller lectins

Elena Shanina, Sakonwan Kuhaudomlarp, Kanhaya Lal, Peter Seeberger,  
Anne Imberty, Christoph Rademacher

► **To cite this version:**

Elena Shanina, Sakonwan Kuhaudomlarp, Kanhaya Lal, Peter Seeberger, Anne Imberty, et al..  
Druggable allosteric sites in  $\beta$ -propeller lectins. *Angewandte Chemie International Edition*, 2021,  
10.1002/anie.202109339 . hal-03412507

**HAL Id: hal-03412507**

**<https://hal.science/hal-03412507>**

Submitted on 3 Nov 2021

**HAL** is a multi-disciplinary open access archive for the deposit and dissemination of scientific research documents, whether they are published or not. The documents may come from teaching and research institutions in France or abroad, or from public or private research centers.

L'archive ouverte pluridisciplinaire **HAL**, est destinée au dépôt et à la diffusion de documents scientifiques de niveau recherche, publiés ou non, émanant des établissements d'enseignement et de recherche français ou étrangers, des laboratoires publics ou privés.

# Druggable allosteric sites in $\beta$ -propeller lectins

Elena Shanina<sup>[a][b]</sup>, Sakonwan Kuhaudomlarp<sup>[e][f][g]</sup>, Kanhaya Lal<sup>[e][h]</sup>, Peter H. Seeberger<sup>[a][b]</sup>, Anne Imberty<sup>[c]</sup> and Christoph Rademacher<sup>[a][b][c][d]\*</sup>

<sup>[a]</sup> Department of Biomolecular Systems, Max Planck Institute of Colloids and Interfaces, , 14476 Potsdam, Germany

<sup>[b]</sup> Department of Chemistry and Biochemistry, Freie Universität Berlin, Arnimallee 22, 14195 Berlin, Germany

<sup>[c]</sup> Department of Pharmaceutical Chemistry University of Vienna Althanstrasse 14, 1080 Vienna, Austria

<sup>[d]</sup> Department of Microbiology, Immunobiology and Genetics Max F. Perutz Labs, 1030 Vienna, Austria

<sup>[e]</sup> University Grenoble Alpes, CNRS, CERMAV 38000 Grenoble, France

<sup>[f]</sup> Department of Biochemistry, Faculty of Science Mahidol University 10400 Bangkok, Thailand

<sup>[g]</sup> Center for Excellence in Protein and Enzyme Technology, Mahidol University 10400 Bangkok, Thailand

<sup>[h]</sup> Dipartimento di Chimica via Golgi 19 Universita' degli Studi di Milano 20133 Milano, Italy

---

**ABSTRACT:** Carbohydrate-binding proteins (lectins) are auspicious targets to combat antimicrobial resistance; however, its non-carbohydrate drug-like inhibitors are still spacious. Here, we present a druggable pocket in a  $\beta$ -propeller lectin BamBL from *Burkholderia ambifaria* as a potential target for allosteric inhibitors. This site was identified employing 19F NMR fragment screening and a computational pocket prediction algorithm SiteMap. The structure-activity relationship study revealed the most promising fragment with a dissociation constant of  $0.3 \pm 0.1$  mM and a ligand efficiency of 0.3 kcal mol<sup>-1</sup>HA-1, which affected the orthosteric site. This effect was substantiated by site-directed mutagenesis in the orthosteric and secondary pockets. Future drug-discovery campaigns that aim to develop small molecule inhibitors can benefit from allosteric sites in lectins as a new therapeutic approach against antibiotic-resistant pathogens

---

## INTRODUCTION

Bacterial infections, especially those involving biofilm formation, are becoming increasingly difficult to treat as antibiotic resistance is rising worldwide. Therefore, identifying new protein targets and anti-adhesives is a promising approach for future treatment of bacterial infections. Since carbohydrate-binding proteins (lectins) are found in many pathogenic microorganisms and involved in host recognition, adhesion and biofilm formation, targeting lectins evolved as an attractive strategy to treat bacterial and fungal infections.<sup>[1]</sup>

Lectins from pathogens often display a high affinity for mammalian carbohydrates, likely deriving from co-evolution.<sup>[2]</sup> Thus, bacteria take advantage of these interactions to adhere and infect the host. A well-known example is the  $\beta$ -propeller lectin BamBL from the Gram-negative bacterium *Burkholderia ambifaria*.<sup>[3]</sup> This opportunistic pathogen belongs to a group of closely related bacterial strains, the *Burkholderia cepacia* complex, causing chronic infections and exhibiting multidrug antibiotic resistance. *B. ambifaria* affects immunocompromised patients as well as those suffering from cystic fibrosis (CF) and can cause pneumonia, respiratory failure and bacteremia.<sup>[4]</sup> Moreover, *B. ambifaria* can promote sporadic outbreaks, but its epidemiology remains elusive.<sup>[5]</sup> Several studies point to an underestimated role of BamBL in affecting host cellular processes,

which go beyond an adhesion to the human lung epithelium.<sup>[6]</sup> Therefore, blocking the carbohydrate-BamBL interactions is a potential avenue to treat chronic infections, but strategies for design of inhibitors are required.

The crystal structure of BamBL revealed that the protein consists of two similar domains and trimerizes to form a 6-bladed  $\beta$ -propeller with 6 fucose-binding sites.<sup>[3]</sup> Bacterial and fungal  $\beta$ -propeller is an efficient carbohydrate-binding fold presenting all binding sites on one face of the donut shape.<sup>[7]</sup> In recent years, several inhibitors for BamBL have been reported. Given the strong affinity of BamBL to  $\alpha$ -L-fucosylated monosaccharides (methyl  $\alpha$ -L-fucopyranoside (MeFuc),  $K_d=1$   $\mu$ M) and complex carbohydrates (H type 2 tetrasaccharide,  $K_d=7.5$   $\mu$ M), the design of inhibitors has been focused on using carbohydrates as a starting point.<sup>[3]</sup> Indeed, this approach has yielded potent BamBL monovalent aryl- $\alpha$ -O-fucoside inhibitors with an affinity comparable to MeFuc.<sup>[8]</sup> Moreover, multivalent compounds with 4 to 6 fucose or aryl- $\alpha$ -O-fucosyl analogues improved selectivity and affinity towards BamBL with  $K_d$  ranging between 10 to 80 nM.<sup>[8a, 9]</sup> However, the main limitation of such complex carbohydrate-based inhibitors is their molecular size. This limits their oral bioavailability and thus complicates the future clinical approval.<sup>[10]</sup> Consequently, small and orally

bioavailable drug-like molecules targeting lectins from pathogens are highly desired, but challenging.

Lectins have been associated with a low druggability index due to their hydrophilic and solvent-exposed carbohydrate-binding sites.<sup>[10-11]</sup> To overcome these limitations, we have previously explored the concept of allosteric modulators for mammalian lectins.<sup>[12]</sup> Allosteric modulators do not bind to the orthosteric (carbohydrate)-binding site, but target an alternative (allosteric) pocket that affects the orthosteric site and *vice versa*. Several druggable, allosteric pockets have been discovered for the mammalian lectins as DC-SIGN (CD209),<sup>[13]</sup> including intra-domain allosteric network that modulates Ca<sup>2+</sup> affinity of Langerin (CD207). This was followed by design of allosteric inhibitors for Langerin supporting the allosteric communication in mammalian lectins.<sup>[12a, 14]</sup> Altogether, these discoveries paved the way for further search of potential allosteric pockets in lectins.

Motivated by previous reports, we assessed the druggability of  $\beta$ -propeller lectins with the focus on a bacterial lectin BambL. Competitive <sup>19</sup>F and T<sub>2</sub>-filtered (CPMG) NMR allowed us to distinguish drug-like fragments binding to lectins in the orthosteric or the secondary sites. To narrow the number of hits, compounds were counter-screened by surface plasmon resonance spectroscopy (SPR) and protein-observed <sup>1</sup>H-<sup>15</sup>N HSQC/TROSY NMR (hereafter, TROSY NMR). The affinity and potential modulatory properties of the most promising hits were derived in three orthogonal NMR experiments (TROSY, PrOF<sup>[15]</sup> and <sup>19</sup>F R<sub>2</sub>-filtered NMR). Finally, computational analysis was applied to predict druggable secondary sites in BambL and validated experimentally by site-directed mutagenesis and NMR.

## RESULTS AND DISCUSSION

### Fragment screening against $\beta$ -propeller lectins

Ligand-observed <sup>19</sup>F and T<sub>2</sub>-filtered (CPMG) NMR are key methods for detection of weak fragment-protein interaction.<sup>[16]</sup> This is owned the T<sub>2</sub> relaxation of the <sup>19</sup>F nucleus, which is highly sensitive to the molecular tumbling changes of the small molecules in the unbound and protein-bound states.<sup>[17]</sup> Therefore, <sup>19</sup>F NMR screening of fragment mixtures is frequently used in drug discovery to estimate the druggability of protein targets. Previously, we successfully applied our diversity-oriented fragment library and <sup>19</sup>F NMR to discover drug-like molecules for mammalian lectins.<sup>[11-12, 13, 18]</sup>

Encouraged by this discovery, we applied this approach to assess the druggability of BambL and related  $\beta$ -propeller lectins as RSL and AFL from bacterium *R. solanacearum* and fungus *A. fumigatus*, respectively (**Figure 1a**). These lectins have sequence and structure similarities with BambL (RSL: 76% sequence identity, RMSD=0.56Å, AFL: 39% sequence identity, RMSD=1.84Å), albeit with different oligomerization for AFL, and both have a low micromolar affinity for terminal  $\alpha$ -L-fucose on animal and plant carbohydrates (AFL:  $K_d$ =76.4  $\mu$ M and RSL:  $K_d$ =0.64  $\mu$ M).<sup>[19]</sup> To assess the druggability of  $\beta$ -propeller lectins, 350 fluorinated fragments were screened in <sup>19</sup>F and CPMG NMR. Herein, we carefully monitored the chemical shift perturbations (CSPs) or a change in peak intensity of <sup>19</sup>F resonances defining CSP>0.01 ppm or peak reduction of 25-

50% as 'high' and 'low' confidence <sup>19</sup>F hits, respectively. In the CPMG NMR spectra, changes in peak intensity of 20-50% or more than 50% were defined as 'low' and 'high' confidence CPMG hits, respectively. Only compounds fulfilling one of three criteria: 1) <sup>19</sup>F hit only, 2) <sup>19</sup>F and CPMG hit and 3) 'high' confidence CPMG hit, were followed up in the counter-screening. As an example, **Figure 1b** shows the identification of the fragment **24** bound to BambL. Such fragments were used to derive a total hit rate. Interestingly,  $\beta$ -propeller lectins showed unusually high hit rates, i.e. 33% and 48% for RSL and AFL/BambL, respectively. Such high total hit rates in a fragment screening suggested either a non-specific binding or the presence of several potentially druggable secondary sites for  $\beta$ -propeller lectins.<sup>[20]</sup> The same library resulted in 10-15% hit rate in previous screenings on C-type lectins, therefore excluding the hypothesis of high hit rates being caused by non-specific frequent hitters<sup>[11, 13]</sup> To further narrow down the number of potential hits, we competed the fragments targeting the orthosteric site using 10 mM MeFuc. Surprisingly, only 2 'low' confidence fragments (<1%) were identified for the orthosteric site of BambL, whereas 17% and 5% of fully or partially competed fragments were observed for AFL and RSL, respectively (fragments **79** and **80**, **Figure 1b**).

To unravel the potential fragment binding sites in  $\beta$ -propeller lectins, we applied a computational pocket prediction algorithm SiteMap<sup>[21]</sup>. Interestingly, SiteMap identified three secondary pockets in the crystal structures of BambL in complex with  $\alpha$ -L-fucose (PDB ID: 3ZW0, **Figure S1**) or H-type 2 tetrasaccharide (PDB ID: 3ZZV),<sup>[3]</sup> as well as in RSL (apo and holo, **Figure S2**). However, shape and size of the predicted sites were slightly different due to differences in residues in the binding sites. Finally, a structurally more distant druggable site was identified for AFL (**Figure S3**). Taken together, high hit rates in <sup>19</sup>F NMR and SiteMap computational pocket prediction analysis strongly suggest the availability of druggable pockets capable of accommodating drug-like molecules in  $\beta$ -propeller lectins.

### Druggable secondary sites in BambL

To explore the concept of secondary sites in  $\beta$ -propeller lectins, we chose BambL as an example. Given a large number of <sup>19</sup>F NMR hits, we focused on 111 fragments with the strongest effects in <sup>19</sup>F and CPMG NMR (**Figure S4a**). Thereby, 13 compounds were removed due to their poor solubility resulting in 98 hits subjected to the orthogonal screening using SPR and TROSY NMR. Briefly, SPR confirmed a dose-dependent interaction of 78 out of 91 fragments with BambL (**Figures 1c** and **S4b**). To further narrow the number of hits, TROSY NMR as a 'gold standard' for hit validation was applied.<sup>[22]</sup> Here, we chose 39 compounds with the strongest effects in <sup>19</sup>F NMR and SPR resulting in 10 hits positive in <sup>19</sup>F NMR, SPR and TROSY NMR (**Figure S4c**). Further, we ranked 10 hits in titration experiments using TROSY NMR, where we performed a partial protein backbone assignment using site-directed mutagenesis as described in the **Supporting information**. Compounds **10**, **12** and **24** promoted the strongest dose-dependent chemical shift perturbations in <sup>15</sup>N BambL (**Figure S5a**). To estimate whether these compounds serve as good starting points for lead development, we derived their affinities ( $K_d$ ) and ligand efficiency (LE)<sup>[23]</sup>. The fragment **24** showed a two-fold stronger affinity

( $K_d=0.4\pm 0.2$  mM, **Figure S5b**) and a better LE value of 0.29 kcal mol<sup>-1</sup>HA<sup>-1</sup> compared to **10** ( $K_d=0.8\pm 0.4$  mM, LE=0.23) and **12** ( $K_d=0.9\pm 0.3$  mM, LE=0.21), which was probably due to its smaller molecular weight. Next, we verified the interaction of BambL with **24** in an orthogonal ligand-observed <sup>19</sup>F R<sub>2</sub>-filtered NMR assay (**Figure S6**), which revealed the similar range  $K_d$

value to that obtained by protein-observed TROSY NMR ( $K_d=0.3\pm 0.1$  mM, LE=0.3 kcal mol<sup>-1</sup> HA<sup>-1</sup>).

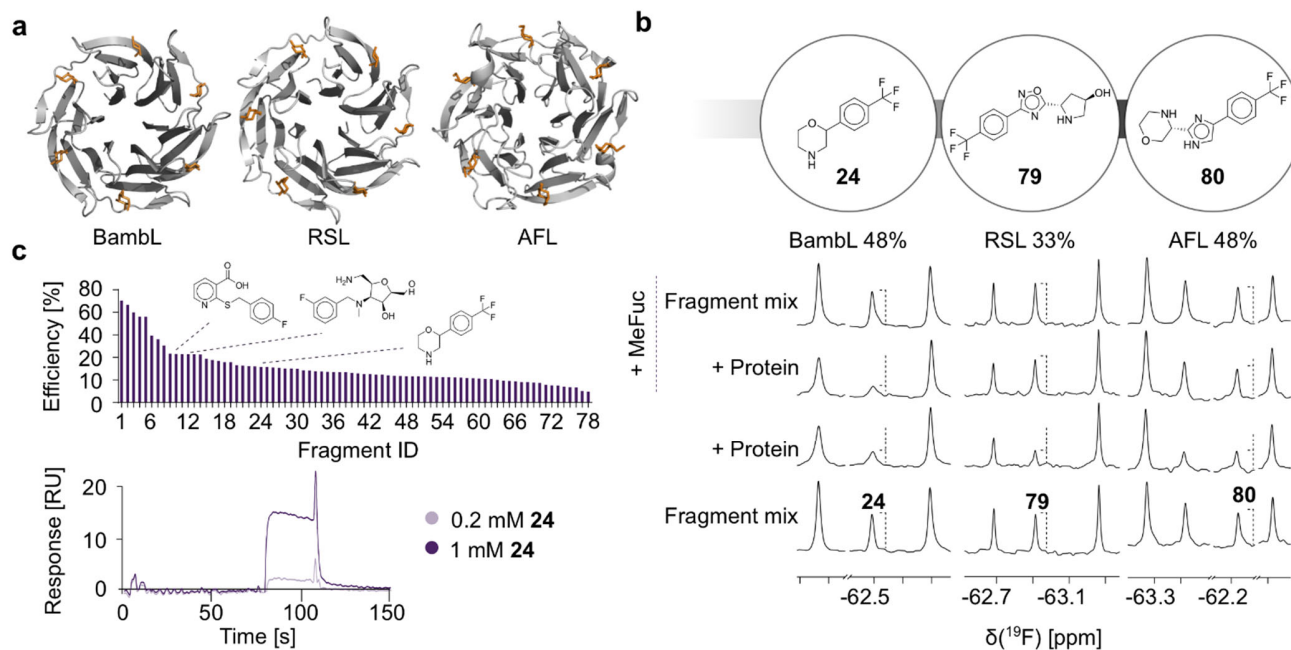


**Figure 1.** Druggability assessment of  $\beta$ -propeller lectins. (a) Cartoon representations of the crystal structures of the  $\beta$ -propeller lectins. Shown are BambL in complex with L-fucose (orange, PDB ID: 3ZZV), RSL (PDB ID: 3ZI8) and AFL (PDB ID: 4AGI). (b) CPMG NMR spectra of fragment mixtures containing 0.05 mM **24**, **79** or **80** show a strong line broadening effect of <sup>19</sup>F resonances (dashed line) in presence of 20  $\mu$ M BambL/AFL and 40  $\mu$ M RSL, whereas only **79** and **80** were competed with 10 mM MeFuc. (c) Shown are the structures of <sup>19</sup>F NMR screening hits for BambL confirmed in SPR and TROSY NMR among 78 hits verified in SPR (top). SPR sensorgram of **24** shows a dose-dependent binding of **24** to BambL (bottom).

To predict the potential binding site of fragment **24** in BambL, three secondary sites identified in SiteMap were investigated for the ability to host the fragment **24**. The predicted sites are located at the interface between the monomers near the C-terminus forming narrow channels (T18, N20, K23, T25, G67, T69, G86 and L87, **Figure S7**) and surrounded by hydrophilic residues, which make them suitable to accommodate ligands with polar groups. As an example, K23 (in three sites) and L87 (in one site) illustrate the differences in side chain orientation, which slightly changes the shape and the size of the predicted sites. Nonetheless, these sites were top ranked by SiteMap for their propensities to harbor drug-like molecules. Although three predicted sites show slight differences in the crystal structure (PDB: 3ZW0), this is only due to differences in side chain orientation in the crystal structure, which are expected to be identical in solution. We selected only one of them for the docking study (**Figure 2a**). Further, we successfully docked **24**, **10** and **12** using Glide (v. 7.8) in the predicted site (**Figures 2b, S7 and S8**). The docking study suggested six

residues (T18, K23, T25, G67, Y84 and L87) to play key role in fragment binding. In particular, **24** bound to the predicted site with nearly identical pose indicating only a minor difference in orientation of morpholine ring in multiple binding poses. Likewise, **12** and **10** were also accommodated in the site showing H-bond interactions with the identified key residues.

To support this prediction experimentally, we quantified the chemical shift perturbations in TROSY NMR spectra of <sup>15</sup>N BambL in presence of fragments **10**, **12** and **24**. Despite only a partial protein backbone assignment, we observed that **10**, **12** and **24** perturbed the same resonances in <sup>15</sup>N BambL. This suggested that fragments targeted identical binding site in BambL, which supports our computational data (**Figures 2c-2e**). Next, we confirmed that **24** bound to a secondary pocket distinct from the orthosteric site. For this, we employed a competitive ligand-observed <sup>19</sup>F CPMG NMR using **24** as a fluorinated reporter and 2-deoxy-2-fluoro-L-fucose (2FF) as a competitor. Compared to MeFuc, 2FF binds to the orthosteric site of BambL with a slightly weaker affinity ( $K_d=18.8\pm 2.3$   $\mu$ M<sup>[24]</sup>) and thus, it

could have a better chance in competing **24**. Indeed, 2FF demonstrated a dose-dependent binding to BamBL with  $IC_{50}$  value of  $0.19 \pm 0.02$  mM being 10-fold weaker than reported previously ( $IC_{50} = 19.9 \mu\text{M}^{[24]}$ , **Figures 2f-g**). Given that 2FF

displaced **24** only partially, we concluded that **24** bound BamBL in the secondary pocket.

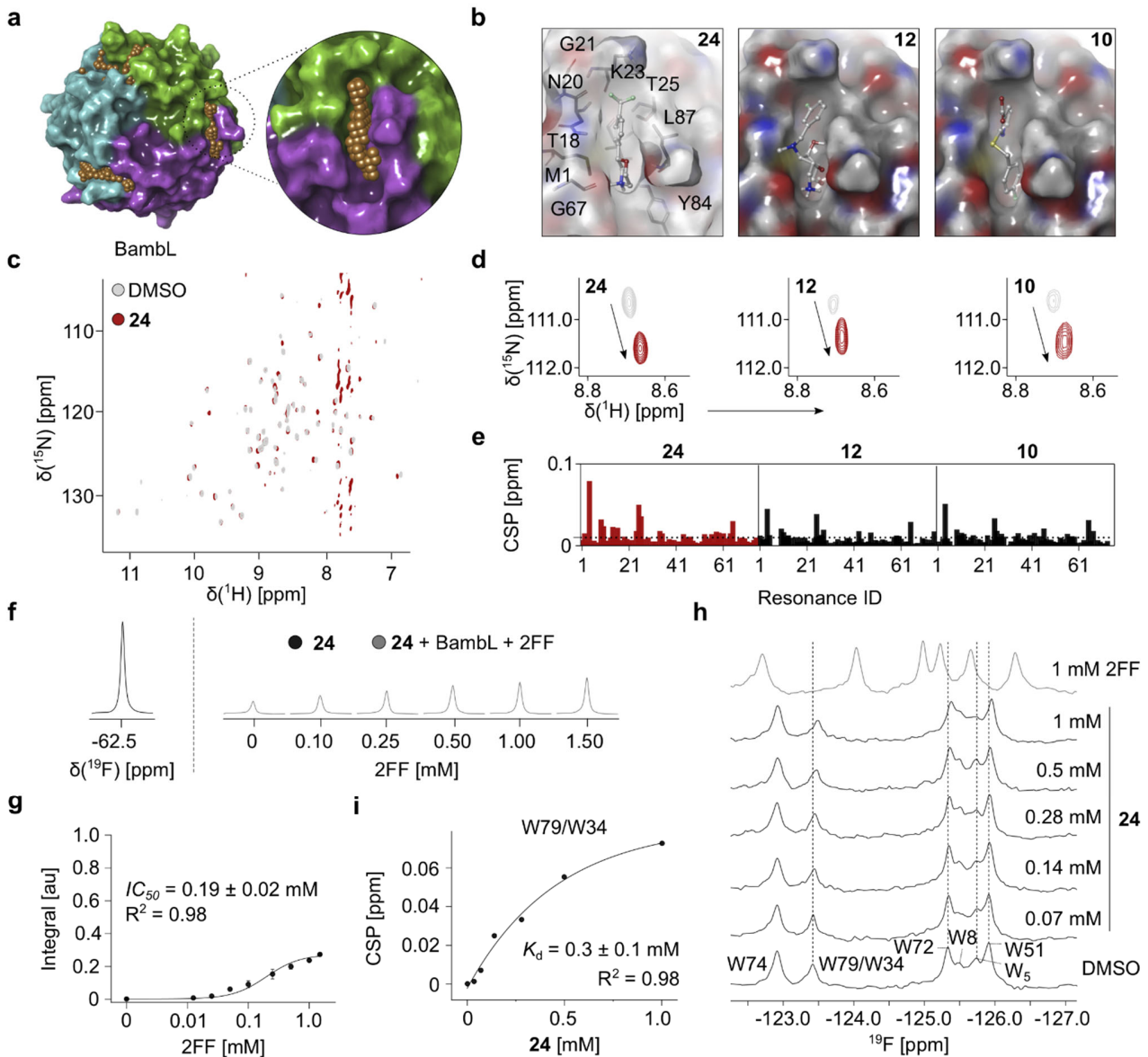


**Figure 2.** Identification of the druggable secondary sites in BamBL. (a) BamBL harbors three potential druggable binding sites, whereas only one secondary site (enlarged view) can accommodate drug-like molecules **24**, **12** and **10** as predicted by SiteMap (PDB ID: 3ZW0). (b) Docking poses of **24**, **12** and **10**. (c) TROSY NMR of  $^{15}\text{N}$  BamBL with DMSO or **24**. (d) Shown is the exemplary resonance perturbed in presence of **24**, **12** and **10**. (e) CSP plots **24**, **12** and **10** demonstrate that fragments perturbed similar resonances in  $^{15}\text{N}$  BamBL, whereas **24** showed a larger magnitude of CSPs compared to **12** and **10**. Dashed line indicates CSPs > 0.01 ppm. (f) and (g) Competitive  $T_2$ -filtered  $^{19}\text{F}$  NMR yielded  $IC_{50}$  value of 2FF in presence of 1 mM **24** and 0.1 mM BamBL. Notably, 2FF competed **24** only partially suggesting **24** bound to BamBL distantly from the orthosteric site. (h) PrOF NMR of 0.1 mM 5FW BamBL shows CSPs of all six 5FW resonances in presence of 1 mM 2FF. Moreover, **24** perturbed W79/W34 ( $W_2$  and  $W_5$ , unassigned), W72 and W51 demonstrating an effect of remote site binders on the carbohydrate-binding site. (i) One-site fit of PrOF NMR titration data. The CSPs of W79/W34 ( $W_2$ ) upon addition of **24** were followed up to derive the affinity.



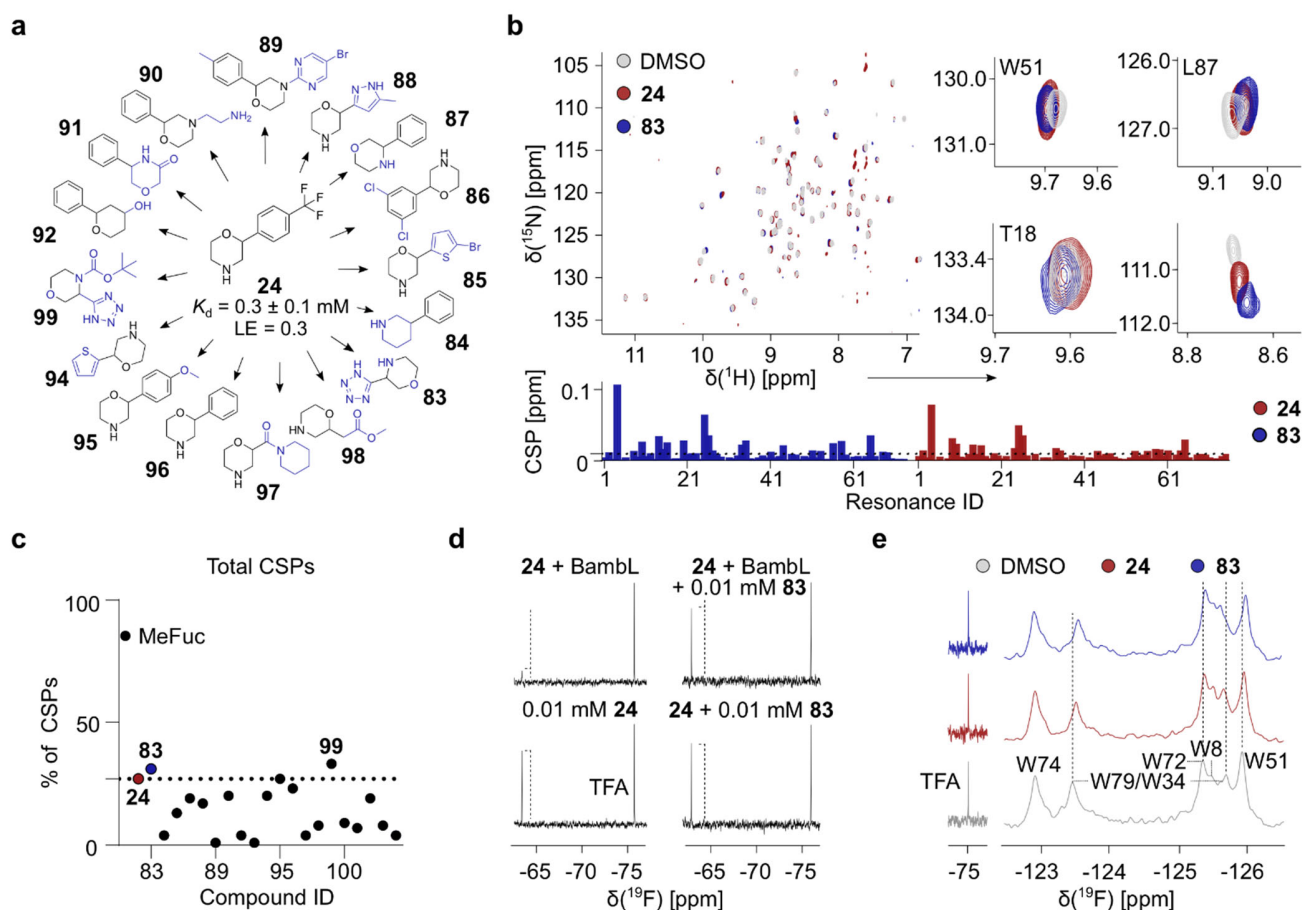


**Figure 3.** Structure activity relationship study of **24**. (a) Shown are 16 out of 22 commercial structural derivatives of **24**, which were ranked using TROSY NMR. (b) TROSY NMR (top panel) of  $^{15}\text{N}$  BamBL in presence of DMSO (gray), **83** (blue) or **24** (red). Qualitative analysis of TROSY NMR (bottom panel). Dashed line indicates CSPs > 0.01 ppm. (c) Total % of CSPs derived in TROSY NMR shows that **83** (31%) and **99** (33%) promoted more CSPs in  $^{15}\text{N}$  BamBL compared to initial hit **24** (dashed line, 27%). (d) 0.1 mM **83** displaced 0.1 mM **24** from its binding site in  $^{19}\text{F}$  CPMG NMR. (e) ProOF NMR of 0.1 mM 5FW BamBL with 1 mM **83** and 1 mM **24**, which showed CSPs of 5FW resonances (dashed line) demonstrating the effect of both fragments on the orthosteric site of 5FW BamBL.

To investigate the impact of **24** binding on the orthosteric site of BamBL, we employed protein-observed  $^{19}\text{F}$  (ProOF) NMR.<sup>[15]</sup> Previously, this method proved to be valuable for identification of small molecules targeting of a bacterial lectin LecA.<sup>[25]</sup> Given that BamBL monomer contains six tryptophan residues in the carbohydrate-binding site (Figure S9a), we sought to apply ProOF NMR to verify the impact of fragment binding on the carbohydrate-binding site. For this, we substituted tryptophan residues in BamBL with 5-fluorotryptophanes (5FW) and assigned four out of six 5FW by site-directed mutagenesis (Figure S9b). Next, we confirmed the activity of 5FW BamBL using MeFuc and 2FF, where all six 5FW resonances showed a slow exchange on the NMR time scale (Figure S9c-S9d). This demonstrated that both natural ligands are strong binders. Thus, ProOF NMR was not well suitable to determine its affinities hampering the accurate derivation of the  $K_d$  values (2FF:  $K_d=46\pm 11\ \mu\text{M}$  compared to reported  $K_d=18.8\pm 2.3\ \mu\text{M}$ ,<sup>[24]</sup> Figure S9e). This is not surprising, given that similar limitations were reported for protein-observed  $^1\text{H}$ - $^{15}\text{N}$  HSQC NMR.<sup>[26]</sup> However, ProOF NMR verified the impact of fragment (**10**, **12** and **24**) binding on the

orthosteric site of 5FW BamBL through W51, W72 and W79/W34 (Figure S10, Table S1). Moreover, titration of **24** to 5FW BamBL perturbed 5FW in a dose-dependent manner delivering a  $K_d$  of  $0.3\pm 0.1\ \text{mM}$  in agreement with our previous results (Figures 2h-2i). Therefore, we investigated whether fragments could inhibit 5FW BamBL interaction with 2FF. Notably, the fragments remained bound to 5FW BamBL in presence of 2FF as shown for **24** and **12** (Figures S9f-S9g). However, the presence of fragments did not inhibit 2FF-5FW BamBL interaction in this assay (**24**:  $K_d=52\pm 3\ \mu\text{M}$ , Figure S9h), which contradicted with our competitive  $^{19}\text{F}$  CPMG NMR and thus, the inhibitory properties of **24** require a further improvement.

Taken together, computational and experimental analyses using  $^{19}\text{F}$  CPMG NMR confirmed the presence of druggable secondary sites in BamBL. Despite the lack of inhibitory properties in ProOF NMR, binding of fragments **10**, **12** and **24** to the secondary site influenced the orthosteric site in BamBL, which strongly suggested the presence of a communication between

the orthosteric and predicted sites. Given this, **24** was subjected to further studies.

### Structure activity relationship of **24**

In our initial SAR study, we aimed to improve the affinity of **24** using commercially available analogues (Table S2, Figure 3a). For this, we employed computational and experimental TROSY NMR analyses. Briefly, we performed TROSY NMR of 16 analogues of **24** (Figure S11), which revealed the importance of the morpholine group in **24** given a fully and partially abrogated binding upon its replacement with piperidine (**84**), morpholine-3-one (**91**) and tetrahydro-2H-pyran-4-ol (**92**) groups, respectively (Figure S12a). Notably, further modification on the amine group to 4-(2-aminoethyl)-morpholine (**90**) was tolerated unlike a more hydrophobic and bulky change as 5-bromopyrimidine (**89**, Figure S12b). Moreover, we observed

that the replacement (**95**) or lack (**96**) of  $\text{CF}_3$  and changing the position of the benzyl group from 1 (**96**) to 2 (**87**) did not abrogate BambL binding (*data not shown*). Therefore, we explored the role of the benzyl group by changing it to 1,3-dichlorobenzene (**86**), 3-methylpyrazole (**88**), methyl acetate (**98**), *N*-formylpiperidine (**97**), tetrazole (**83**), 2-bromo- (**85**) or thiophene (**94**). As result, analogues **83**, **85**, **86**, **88**, and **94** preserved binding to  $^{15}\text{N}$  BambL (Figures S13a and 3b). As only **83** promoted more total CSPs above 0.01 ppm in  $^{15}\text{N}$  BambL compared to the initial scaffold **24**, we confirmed it in a competitive  $^{19}\text{F}$  CPMG NMR (Figure 3c). Evidently,  $10\ \mu\text{M}$  **24** was fully competed by  $10\ \mu\text{M}$  **83** showing that both fragments targeted the same druggable pocket in BambL (Figure 3d).

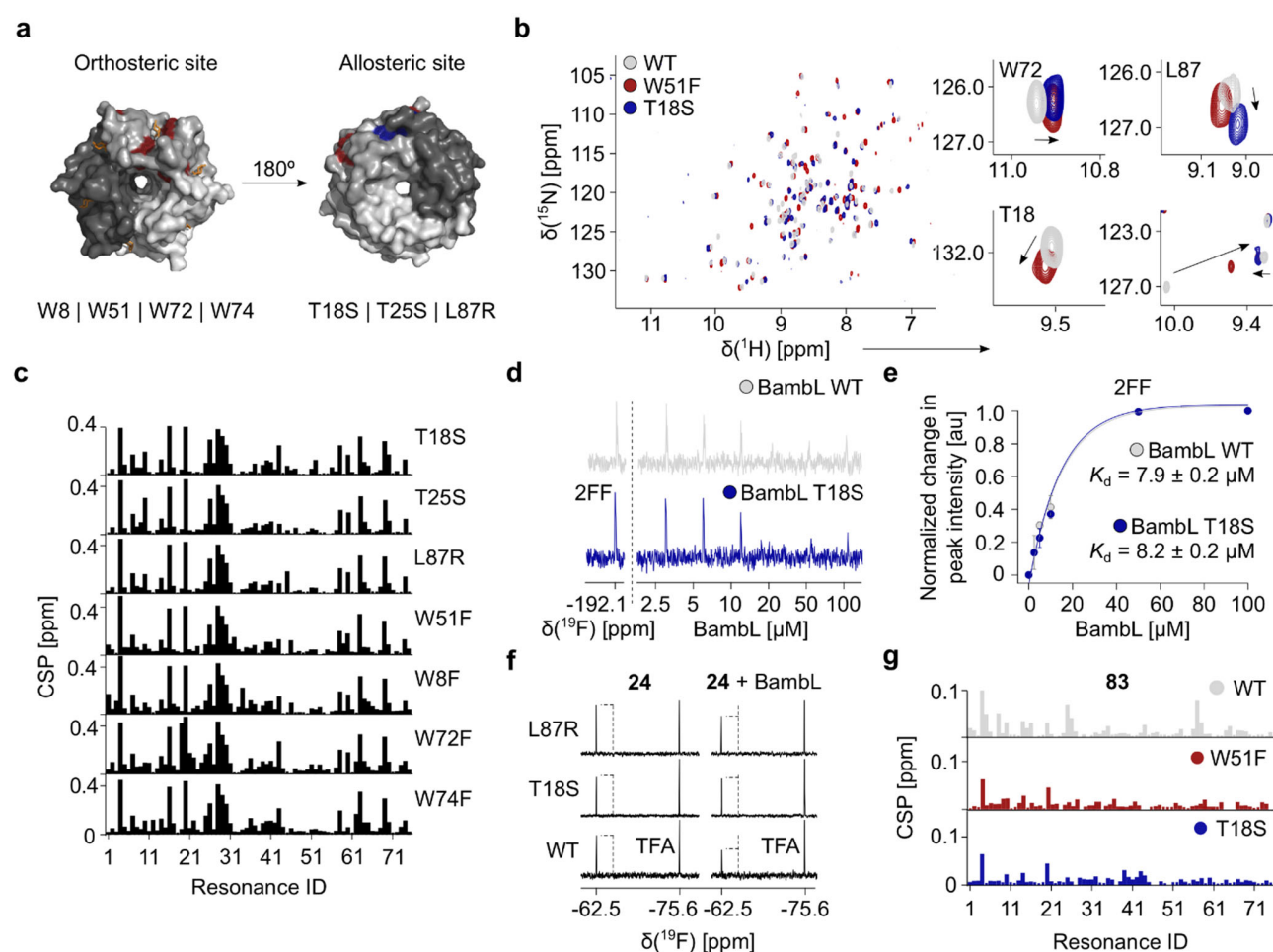


**Figure 4.** Characterization of the secondary site in BambL. (a) Top and bottom views on the orthosteric (red) and potential allosteric site (blue) in the crystal structure of BambL in complex with L-fucose (orange, PDB ID: 3ZZV). Single-point mutations in the orthosteric and secondary site have been proposed to check the communication between the two sites. (b) Overlay of  $^{15}\text{N}$  TROSY NMR spectra of BambL WT, W51F and T18S shows the conformational changes introduced by both site-directed mutations. Notably, W51F and T18S mutations promoted identical changes on other resonances in the orthosteric (W72) and secondary sites (L87R) in BambL. (c) CSP studies of mutant apo forms compared to BambL WT show a preserved CSP pattern in both tryptophan and allosteric pocket mutants. (d)  $^{19}\text{F}$  NMR spectra of 2FF in presence of BambL WT and T18S. (e) Determination of 2FF  $K_d$  values for BambL T18S revealed a preserved affinity compared to BambL WT. (f)  $^{19}\text{F}$  CPMG NMR of **24** with BambL WT, T18S and L87R to verify its binding site. (g) Binding of **83** to W51F and T18S promoted less CSPs compared to WT supporting the existence of a communication between the orthosteric and the remote sites

Next, we validated five commercially available analogues of **83** in TROSY NMR (**99-104**, **Table S2**). Compounds **100** and **104** proved the importance of the tetrazole and morpholine groups for binding of **83** to the secondary site given the lack of binding in TROSY NMR. Similar to **90**, the presence of a substituent (tert-butyl formate, **99**) on a nitrogen atom of morpholine group was tolerated well and thus, this position could serve for future fragment growing (**Figure S13b**).

Computational docking analysis of four derivatives of compounds **24** (**83**, **84**, **87**, **90** and **94**) was performed to check if the predicted pocket could accommodate these compounds (**Figure S14**). Hereby, we chose these fragments to check the importance of morpholine and benzyl groups. As result, all compounds could be accommodated in the site, whereas **84** did not form electrostatic interactions. These observations were in agreement with our experimental data showing the importance of the morpholine group in **24** as shown for **87**, whereas other parts of the compound are rather interchangeable (e.g. **83** and **94**). Finally, we confirmed that the analogue **83** could affect the carbohydrate-binding site of 5FW BamBL in PrOF NMR (**Figure 3e**). Indeed, **83** perturbed W79/W34, W51 and W72 similar to the initial hit **24** causing even larger NMR chemical shift perturbations of 5FW resonances.

Taken together, our SAR study confirmed the presence of a druggable secondary site in BamBL. Moreover, binding of two fragments with a similar scaffold (**24** and **83**) to the secondary pocket affected the orthosteric site of BamBL suggesting a communication between both sites.

#### *Communication between the carbohydrate and remote sites in BamBL*

To further prove allosteric communication in BamBL, we proposed that mutations in the orthosteric and secondary sites could introduce perturbations that propagate through the network and result in similar chemical shift changes. For this, we used four (W8F, W51F, W72F and W74F) and three (T18S, T25S and L87R) mutants for the orthosteric and predicted remote sites, respectively (**Figure 4a**). All mutants were folded and active as observed by TROSY NMR (**Figure S15**). Next, we quantified and compared the NMR chemical shift perturbations (CSPs) induced by mutations in their apo forms with respect to the wild type (WT). Interestingly, perturbations were not restricted to residues in the close periphery, but also affected remote residues, as shown for W51F and T18S mutants. Here, we clearly identified a chemical shift perturbation of W72 in both WT and T18S mutants moving along the same vector (**Figure 4b**). Quantification of NMR chemical shift perturbations of the apo WT to other apo mutant forms (W8F, W72F, W74F, L87R and T18S) revealed the conformational changes through the same paths in  $^{15}\text{N}$  BamBL, which is typical for allosteric proteins (**Figure 4c**).<sup>[27]</sup> To assess if mutations in the predicted pocket alter the affinity of proteins to the natural carbohydrates, we titrated 2FF and a complex carbohydrate (F-H type 2) to BamBL WT and T18S (**Figures 4d** and **S16a**). Compared to BamBL WT, T18S preserved its affinity for 2FF (**Figure 4e**, WT:  $K_d=7.9\pm 0.2\ \mu\text{M}$ , T18S:  $K_d=8.2\pm 0.2\ \mu\text{M}$ ). However, BamBL T18S showed nearly two-fold decrease in affinity for a complex carbohydrate, F-H type 2 (**Figure S16b**,  $K_d=16.7\pm 2.5$

$\mu\text{M}$ ) compared to BamBL WT ( $K_d=9\pm 2\ \mu\text{M}$ <sup>[28]</sup>). To verify the binding epitope of F-H type 2 to  $^{15}\text{N}$  BamBL T18S, we used TROSY NMR and compared it to WT (**Figure S16c**). Overall, T18S mutation reduced the magnitude of CSPs in  $^{15}\text{N}$  BamBL suggesting a negative modulatory role of the pocket on the carbohydrate-binding site in recognizing complex carbohydrates (**Figure S16d**). Interestingly, a discrepancy between two carbohydrate-binding sites in the interaction with the complex carbohydrates, but not with MeFuc, has been reported for BamBL recently.<sup>[9a]</sup> Given the lack in affinity change with 2FF, we propose that inhibition of secondary site could potentially down-regulate the affinity of BamBL by tuning the orthosteric site between two monomers, but not within a monomer. However, this hypothesis requires further investigations.

Finally, we examined the impact of the pocket mutations on binding of the most potent fragments **24** and **83** by  $^{19}\text{F}$  CPMG and TROSY NMR. Notably, pocket mutations reduced **24** binding in  $^{19}\text{F}$  CPMG (**Figure 4f**) and TROSY NMR experiments (**Figures S17a-S17b**) allowing us to conclude that the mutations blocked the entrance into the predicted pocket only partially. Similarly, we observed this effect with the fragment **83** (**Figures S18a**), which is in agreement with the computational docking analysis suggesting the presence of two orientations for **83** and its derivative **99** (**Figure S19**). Interestingly, mutation in the orthosteric site (W51F) reduced **83** binding similarly to  $^{15}\text{N}$  BamBL T18S and other pocket mutants (**Figures 4g** and **S18b**), which confirms the ‘end-to-end’ communication of both sites.

Taken together, these data reveal the existence of a druggable allosteric site in BamBL. The NMR chemical shift perturbations of backbone resonances of  $^{15}\text{N}$  BamBL pocket mutants are located in sites distal to the actual pocket and the communication extends to the carbohydrate recognition site, suggesting a propagation of conformational changes in BamBL upon changes in the allosteric pocket.

## Conclusion

We report the presence of druggable pockets in a bacterial  $\beta$ -propeller lectin BamBL, which could be used to design allosteric inhibitors. We showed binding of fragments to BamBL in a  $^{19}\text{F}$  NMR screening and validated hits using orthogonal methods: SPR and TROSY NMR. Computational pocket prediction analysis SiteMap identified three potential druggable pockets in BamBL trimer. We also showed that the potential secondary binding sites could accommodate drug-like molecules (**24**, **10** and **12**). Initial SAR study of **24** ( $K_d=0.3\pm 0.1\ \text{mM}$ ,  $\text{LE}=0.3$ ) proved the pocket identity by confirming the predicted part of **24** scaffold responsible for its binding to the pocket in our docking study. Notably, fragment binding to the secondary site induced conformational changes in the carbohydrate-binding site of 5FW BamBL in PrOF NMR. This observation allowed us to propose the presence of a communication between two spatially distant binding sites in BamBL. Employing site-directed mutagenesis within the predicted and orthosteric sites, we observed conformational changes of  $^{15}\text{N}$  BamBL backbone resonances in TROSY NMR in distal regions from the mutation sites. Such behavior is typical for allosteric proteins. Given a fungal AFL and bacterial RSL lectins show similarities to BamBL in structure, hit rates and secondary pockets, we believe the allostery



could also be present in other  $\beta$ -propeller lectins. These observations will support future drug-discovery campaigns that aim to develop drug-like allosteric inhibitors for bacterial and fungal lectins.

## Acknowledgements

We thank the Max Planck Society and German Research Foundation (DFG) [RA1944/7-1] for supporting this work, which was in the scope of German Research Foundation and French National Research Agency [ANR-17-CE11-0048] project 'Glycomime'. The authors acknowledge support by the H2020 PhD4Glycodrug program (MSCA 76558), ANR PIA Glyco@Alps (ANR-15-IDEX-02) and Labex Arcane/CBH-EUR-GS (ANR-17-EURE-0003).

## References

- [1] <sup>a</sup>L. C. Breitenbach Barroso Coelho, P. Marcelino dos Santos Silva, W. Felix de Oliveira, M. C. de Moura, E. Viana Pontual, F. Soares Gomes, P. M. Guedes Paiva, T. H. Napoleão, M. T. dos Santos Correia, *Journal of Applied Microbiology* **2018**, *125*, 1238-1252; <sup>b</sup>J. Meiers, E. Siebs, E. Zahorska, A. Titz, *Current opinion in chemical biology* **2019**, *53*, 51-67.
- [2] J. R. Bishop, P. Gagneux, *Glycobiology* **2007**, *17*, 23r-34r.
- [3] A. Audfray, J. Claudinon, S. Abounit, N. Ruvoën-Clouet, G. Larson, D. F. Smith, M. Wimmerová, J. Le Pendu, W. Römer, A. Varrot, A. Imberty, *The Journal of biological chemistry* **2012**, *287*, 4335-4347.
- [4] <sup>a</sup>K. A. Ramsay, C. A. Butler, S. Paynter, R. S. Ware, T. J. Kidd, C. E. Wainwright, S. C. Bell, *Journal of clinical microbiology* **2013**, *51*, 3975-3980; <sup>b</sup>G. A. Pradenas, B. N. Ross, A. G. Torres, *Vaccines* **2016**, *4*.
- [5] <sup>a</sup>E. C. Nannini, A. Ponessa, R. Muratori, P. Marchiaro, V. Ballerini, L. Flynn, A. S. Limansky, *The Brazilian journal of infectious diseases : an official publication of the Brazilian Society of Infectious Diseases* **2015**, *19*, 543-545; <sup>b</sup>T. Coenye, E. Mahenthalingam, D. Henry, J. J. LiPuma, S. Laevens, M. Gillis, D. P. Speert, P. Vandamme, *International journal of systematic and evolutionary microbiology* **2001**, *51*, 1481-1490.
- [6] I. Wilhelm, E. Levit-Zerdoun, J. Jakob, S. Villringer, M. Frensch, R. Übelhart, A. Landi, P. Müller, A. Imberty, R. Thuenuer, J. Claudinon, H. Jumaa, M. Reth, H. Eibel, E. Hobeika, W. Römer, *Science Signaling* **2019**, *12*, eaao7194.
- [7] F. Bonnardel, A. Kumar, M. Wimmerova, M. Lahmann, S. Perez, A. Varrot, F. Lisacek, A. Imberty, *Structure* **2019**, *27*, 764-775.e763.
- [8] <sup>a</sup>D. Goyard, V. Baldoneschi, A. Varrot, M. Fiore, A. Imberty, B. Richichi, O. Renaudet, C. Nativi, *Bioconjugate Chemistry* **2018**, *29*, 83-88; <sup>b</sup>B. Richichi, A. Imberty, E. Gillon, R. Bosco, I. Sutkeviciute, F. Fieschi, C. Nativi, *Organic & biomolecular chemistry* **2013**, *11*, 4086-4094.
- [9] <sup>a</sup>S. Kuhaudomlarp, L. Cerofolini, S. Santarsia, E. Gillon, S. Fallarini, G. Lombardi, M. Denis, S. Giuntini, C. Valori, M. Fragai, A. Imberty, A. Dondoni, C. Nativi, *Chemical science* **2020**, *11*, 12662-12670; <sup>b</sup>N. Galanos, Y. Chen, Z. P. Michael, E. Gillon, J.-P. Dutasta, A. Star, A. Imberty, A. Martinez, S. Vidal, *ChemistrySelect* **2016**, *1*, 5863-5868; <sup>c</sup>C. Ligeour, A. Audfray, E. Gillon, A. Meyer, N. Galanos, S. Vidal, J.-J. Vasseur, A. Imberty, F. Morvan, *RSC Advances* **2013**, *3*, 19515-19524.
- [10] B. Ernst, J. L. Magnani, *Nature reviews. Drug discovery* **2009**, *8*, 661-677.
- [11] J. Aretz, E.-C. Wamhoff, J. Hanske, D. Heymann, C. Rademacher, *Frontiers in Immunology* **2014**, *5*.
- [12] <sup>a</sup>J. Aretz, U. R. Anumala, F. F. Fuchsberger, N. Molavi, N. Ziebart, H. Zhang, M. Nazaré, C. Rademacher, *Journal of the American Chemical Society* **2018**, *140*, 14915-14925; <sup>b</sup>B. G. Keller, C. Rademacher, *Current opinion in structural biology* **2020**, *62*, 31-38.
- [13] J. Aretz, H. Baukman, E. Shanina, J. Hanske, R. Wawrzinek, V. A. Zapol'skii, P. H. Seeberger, D. E. Kaufmann, C. Rademacher, *Angewandte Chemie International Edition* **2017**, *56*, 7292-7296.
- [14] <sup>a</sup>T. T. Waldron, T. A. Springer, *Proceedings of the National Academy of Sciences of the United States of America* **2009**, *106*, 85-90; <sup>b</sup>J. Hanske, S. Aleksic, M. Ballaschk, M. Jurk, E. Shanina, M. Beerbaum, P. Schmieder, B. G. Keller, C. Rademacher, *Journal of the American Chemical Society* **2016**, *138*, 12176-12186.
- [15] C. T. Gee, K. E. Arntson, A. K. Urick, N. K. Mishra, L. M. Hawk, A. J. Wisniewski, W. C. Pomerantz, *Nature protocols* **2016**, *11*, 1414-1427.
- [16] C. R. Buchholz, W. C. K. Pomerantz, *RSC Chemical Biology* **2021**.
- [17] C. Dalvit, A. Vulpetti, *Journal of medicinal chemistry* **2019**, *62*, 2218-2244.
- [18] <sup>a</sup>J. Aretz, Y. Kondoh, K. Honda, U. R. Anumala, M. Nazaré, N. Watanabe, H. Osada, C. Rademacher, *Chemical communications (Cambridge, England)* **2016**, *52*, 9067-9070; <sup>b</sup>J. Schulze, H. Baukman, R. Wawrzinek, F. F. Fuchsberger, E. Specker, J. Aretz, M. Nazaré, C. Rademacher, *ACS chemical biology* **2018**, *13*, 3229-3235.
- [19] <sup>a</sup>N. Kostlánová, E. P. Mitchell, H. Lortat-Jacob, S. Oscarson, M. Lahmann, N. Gilboa-Garber, G. Chambat, M. Wimmerová, A. Imberty, *Journal of Biological Chemistry* **2005**, *280*, 27839-27849; <sup>b</sup>J. Houser, J. Komarek, N. Kostlanova, G. Cioci, A. Varrot, S. C. Kerr, M. Lahmann, V. Balloy, J. V. Fahy, M. Chignard, A. Imberty, M. Wimmerova, *PLOS ONE* **2013**, *8*, e83077.
- [20] R. F. Ludlow, M. L. Verdonk, H. K. Saini, I. J. Tickle, H. Jhoti, *Proceedings of the National Academy of Sciences* **2015**, *112*, 15910-15915.
- [21] T. A. Halgren, *J Chem Inf Model* **2009**, *49*, 377-389.
- [22] A. D. Gossert, W. Jahnke, *Progress in nuclear magnetic resonance spectroscopy* **2016**, *97*, 82-125.
- [23] A. L. Hopkins, C. R. Groom, A. Alex, *Drug discovery today* **2004**, *9*, 430-431.
- [24] T. Dingjan, É. Gillon, A. Imberty, S. Pérez, A. Titz, P. A. Ramsland, E. Yuriev, *Journal of Chemical Information and Modeling* **2018**, *58*, 1976-1989.
- [25] E. Shanina, E. Siebs, H. Zhang, D. Varón Silva, I. Joachim, A. Titz, C. Rademacher, *Glycobiology* **2020**, *31*, 159-165.
- [26] M. P. Williamson, *Progress in nuclear magnetic resonance spectroscopy* **2013**, *73*, 1-16.
- [27] D. D. Boehr, J. R. Schnell, D. McElheny, S.-H. Bae, B. M. Duggan, S. J. Benkovic, H. J. Dyson, P. E. Wright, *Biochemistry* **2013**, *52*, 4605-4619.
- [28] G. Fittolani, E. Shanina, M. Guberman, P. H. Seeberger, C. Rademacher, M. Delbianco, *Angewandte Chemie International Edition* **2021**, *60*, 13302-13309.